Oncogene (2016) **35,** 4689–4697

www.nature.com/onc

ORIGINAL ARTICLE

BET bromodomain inhibitors synergize with ATR inhibitors to induce DNA damage, apoptosis, senescence-associated secretory pathway and ER stress in Myc-induced lymphoma cells

SV Muralidharan[1], J Bhadury[1], LM Nilsson[1], LC Green[1], KG McLure[2,3] and JA Nilsson[1]

Inhibiting the bromodomain and extra-terminal (BET) domain family of epigenetic reader proteins has been shown to have potent anti-tumoral activity, which is commonly attributed to suppression of transcription. In this study, we show that two structurally distinct BET inhibitors (BETi) interfere with replication and cell cycle progression of murine Myc-induced lymphoma cells at sub-lethal concentrations when the transcriptome remains largely unaltered. This inhibition of replication coincides with a DNA-damage response and enhanced sensitivity to inhibitors of the upstream replication stress sensor ATR *in vitro* and in mouse models of B-cell lymphoma. Mechanistically, ATR and BETi combination therapy cause robust transcriptional changes of genes involved in cell death, senescence-associated secretory pathway, NFkB signaling and ER stress. Our data reveal that BETi can potentiate the cell stress and death caused by ATR inhibitors. This suggests that ATRi can be used in combination therapies of lymphomas without the use of genotoxic drugs.

Oncogene (2016) **35,** 4689–4697; doi:10.1038/onc.2015.521; published online 25 January 2016

INTRODUCTION

Epigenetic readers of acetylated histones, such as bromodomain and extra-terminal (BET) proteins (Brd2, Brd3, Brd4 and BrdT), have recently emerged as promising targets of anti-cancer drugs. BET proteins have a vital role in transcription of genes involved in cell cycle regulation and apoptosis.[1] The mode of action has been linked to the ability of Brd2 to bind E2F[2,3] and Brd4 to bind pTEFb.[4,5] The latter binding enables Cdk9 in pTEFb to phosphorylate the C-terminal domain of RNA polymerase II, which results in elongation at transcription pause sites.[6] Recruitment of pTEFb by Brd4 can also regulate pause release of downstream genes, thereby operating as enhancers.[7]

Small molecule inhibitors of BET proteins (BETi) occupy the acetyl-binding pockets of one or both of the two bromodomains present in each BET protein, and have been shown to induce growth arrest and apoptosis in a wide variety of hematologic and solid tumor cells.[1] In some malignancies the anti-proliferative effects correlate with downregulation of *MYC* or *MYCN*,[8–18] as these are often regulated by transcription pause release.[19,20] Using two structurally unrelated BETi, JQ1 and RVX2135, we recently demonstrated that BETi can suppress cell cycle progression and induce apoptosis in transgenic murine Myc-induced lymphoma without suppressing *Myc*.[21] Moreover, we demonstrated that BET inhibition also results in induction of silenced and stress-induced genes, a feature shared by histone deacteylase inhibitors. Indeed we, and others, have shown that BETi and HDACi synergize to kill lymphoma cells.[21,22] These studies suggest that targeting multiple epigenetic regulators in cancer cells has therapeutic potential.

BET inhibition causes profound effects on the transcriptome in lymphoma cells resulting in cell death. We previously observed that at lower concentrations BETi cells did not die but proliferated more slowly.[21] Here we demonstrate that BETi inhibits S-phase progression and S-phase entry in a concentration-dependent manner. This correlates with an enhanced sensitivity to the inhibition of ATR, a checkpoint kinase that is essential for monitoring replication. The novel ATR inhibitor, AZ20 can synergize *in vitro* and *in vivo* with RVX2135 by enhancing cell death and tumor regression.

RESULTS

BETi blocks progression into and through S-phase

Our recent study demonstrated that the BETi JQ1 and RVX2135 are capable of displacing BET proteins from chromatin and killing lymphoma cells at concentrations that globally suppress transcription.[21] We also observed that at a 10-fold lower concentration, BETi significantly suppressed cell growth without killing the cells. To investigate this observation in more detail we measured thymidine incorporation and performed cell cycle analyses using flow cytometry. The cell cycle distribution on DNA histograms shows subtle reduction in the S-phase at lower concentrations of BETi, but thymidine incorporation is markedly suppressed (Figure 1a). Moreover, Geminin, a protein that accumulates in S-phase, maintains its expression in cells treated with low-dose BETi (Figure 1b). However at higher concentrations of BETi, the cells are unable to enter S-phase as evident by flow

[1]Department of Surgery, Sahlgrenska Cancer Center, Institute of Clinical Sciences, Sahlgrenska Academy, University of Gothenburg, Gothenburg, Sweden and [2]Zenith Epigenetics Corp, Calgary, Alberta, Canada. Correspondence: Professor JA Nilsson, Department of Surgery, Sahlgrenska Cancer Center, Institute of Clinical Sciences, Sahlgrenska Academy, University of Gothenburg, Medicinaregatan 1G, Plan 6 SE-405 30, 41390 Gothenburg, Sweden.
E-mail: jonas.a.nilsson@surgery.gu.se
[3]Present address: Ermaris Bio Corp, Calgary, Alberta, Canada.
Received 20 August 2015; revised 8 November 2015; accepted 11 December 2015; published online 25 January 2016

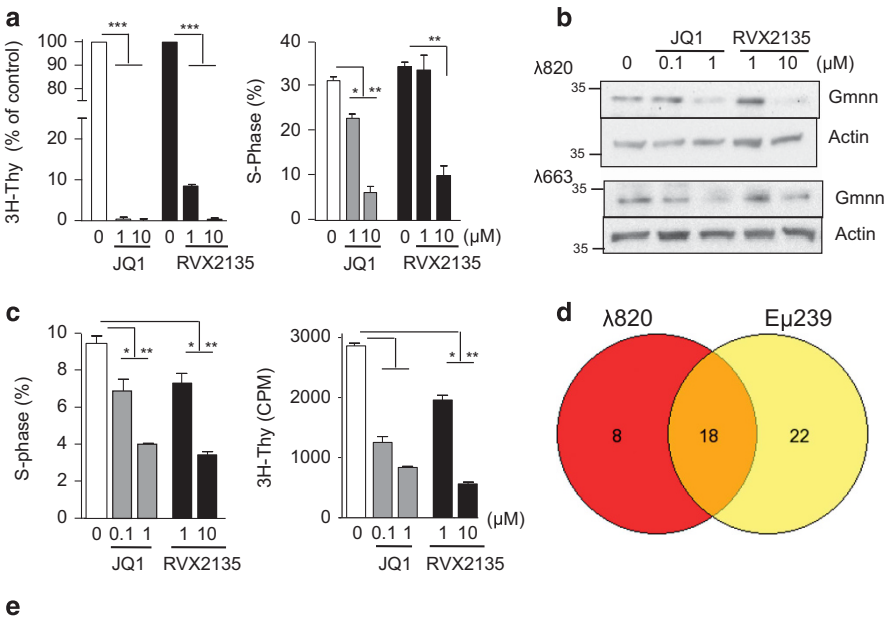

e

Target	Compound
Aurora	CYC116, ENMD-2076, MLN8237, VX-680
CDK	AT7519, PHA-793887
mTOR	AZD8055, KU-0063794
mTOR/PI3K	BEZ235, GDC-0980, GSK1059615
PI3K	BKM120, GSK2126458, PKI587
Single hits	RAF265 (BRAF/VEGF), KX2-391(SRC), TG101209 (JAK), NPI-2358 (VDA)

Figure 1. BETi inhibit S-phase progression and synergize with cell cycle inhibitors. (**a**) λ820 murine Myc-induced lymphoma cells were treated with vehicle (DMSO) or treated with 0.1 μM or 1 μM of JQ1, or 1 μM or 10 μM of RVX2135 for 24 h. The cells were labeled with ^{3}H-thymidine during the final 4 h of treatment and incorporation was measured by scintillation (left). Treated cells were also lysed and their nuclei stained with 7-AAD, followed by flow cytometry measuring the DNA content (right). Shown are quantifications of cells in the S-phase gate. (**b**) Western blotting analysis of lysates from vehicle-treated or BETi-treated λ820 or λ663 cells with antibodies directed against the S-phase marker Geminin and β-actin (as a loading control). (**c**) P493-6 cells were treated with tetracycline for 72 h, after which they were released from tetracycline-mediated repression for 24 h. BETi at the indicated concentrations were added 4 h after turning Myc on. The cells were analyzed either for DNA content (left) or for thymidine incorporation (right) to assess entry into S-phase. (**d**) λ820 and Eμ239 cells were cultured in the presence vehicle (DMSO) or 100 nM JQ1 in 96-well plates where each individual well contained vehicle or 1 μM of a small molecule inhibitor (150 different). After 48 h, plates were analyzed for viability with Cell-Titer-Glo. Shown is a Venn diagram comparing compounds that synergize with JQ1 in both λ820 and Eμ239 cells. (**e**) List of compounds that show synergy in both cell lines.

cytometry and the absence of Geminin expression and thymidine incorporation (Figures 1a and b). At high concentrations of BETi a global suppression of gene transcription can be observed, which is not observed in cells treated with lower concentrations (Supplementary Figure S1), despite the cells being growth-impaired.

These data suggest that a lower concentration of BETi leads to slower progression through S-phase, whereas at higher concentrations, entry of cells into S-phase is blocked. To test this in a synchronized system we used a human B-cell line, P493-6, which carries an episome containing a tetracycline-regulated (TET-OFF) *MYC* transgene.[23] These cells express high levels of c-Myc when cultured in regular B-cell media but addition of tetracycline represses *MYC*, leading to the accumulation of cells in G1. This G1 arrest is reversible by washing cells in tetracycline-free media, allowing the cells to re-enter the cell cycle in a synchronous manner. To study the impact of BET inhibition on the entry of cells into the cell cycle, P493-6 cells were released from tetracycline-suppression of *MYC* in the presence or absence of high or low concentrations of BETi. Similar to murine lymphoma cells expressing *MYC* from a transgenic construct, BETi does not suppress *MYC* expression in P493-6 (Supplementary Figures S2a and b). Consistent with data from λ820 cells, low concentration of BETi results in slowed progression through S-phase, whereas high concentrations of BETi prevent cell cycle entry, as shown by cell cycle distribution determined by flow cytometry and by ^{3}H-thymidine incorporation (Figure 1c and Supplementary Figure S2c). This suppression of replication was not observed in a cell-free replication system, where BETi does not hamper the replication of plasmids containing an SV40 origin of replication (Supplementary Figure S2d). Therefore BETi exerts an effect on chromatin or regulation of replication to inhibit S-phase progression rather than on the replication process *per se*.

BETi sensitize cells to inhibitors of ATR

The observation that lower concentrations of BETi only results in slowed progression through S-phase, but not apoptosis[21] prompted the question of whether there are active pathways that maintain viability in these cells. To answer that, we used a small molecule pharmacogenetic library composed of 150 clinically relevant inhibitors of various target molecules that we have used in previous drug screens.[24] λ820 and Eμ239 cells were

treated with the small molecule library in the presence or absence of 100 nM JQ1 to identify compounds that can synergize with BETi (Figures 1d and e). Two classes of compounds stand out in their ability to synergize with BETi: Aurora kinase inhibitors and PI3K/mTOR inhibitors. Notably though, the JAK inhibitor TG101209 has recently been shown to be a potent BETi,[25,26] suggesting that the synergy is only owing to an enhancement of BET inhibition which eventually results in cell death.[21] Aurora kinase inhibitors could be reasoned to synergize because of the role of BET proteins in mitosis.[27] Lastly, there is an intriguing possibility that the synergistic effect of BETi/PI3K/mTOR inhibitors may partly be owing to the fact that the compounds at 1 μM may inhibit several members of the same kinase family, the PI3K-like family (PIKK). In view of the findings that BETi blocked progression through S-phase (Figure 1), and because off-target effects had been overlooked in previous studies describing BETi synergies with P13K/mTOR inhibitors[28,29] we decided to investigate the possibility of multiple kinase targeting of the identified screening hits.

The PIKK-like family of kinases includes PI3K, mTOR and the DNA-damage response kinases ATM, ATR and DNA-PK. ATR is a critical regulator of DNA replication during replication stress, a scenario that can be caused by stalled replication forks or oncogenes such as Myc.[30] We, and others, have previously shown that Myc-driven lymphomas are sensitive to inhibitors of ATR or the downstream ATR phosphorylation target and signaling mediator Chk1.[31–34] In view of this and the fact that BETi appeared to impact replication (Figure 1 and Supplementary Figure S2), it was of particular interest that one of the PIKK inhibitors in our library, NVP-BEZ235 (BEZ235; Figure 2a), has been shown to not only inhibit PI3K/mTOR but also ATR, ATM and DNA-PK.[35,36]

To investigate if replication master regulator ATR could be the target whose inhibition synergized with BETi we assessed the effect of different phosphorylation targets of two selective ATR inhibitors (VE-821 and AZ20) and two PI3K/mTOR inhibitors found to synergize with low-dose BETi (BEZ235 and GSK1059615). As expected, both the selective ATR inhibitors inhibited phosphorylation of Chk1, induced phosphorylation of ATM target H2Ax (γH2Ax) suggesting induction of DNA double-strand breaks, but did not suppress phosphorylation of mTOR target 4EBP1 (Figure 2b). The PI3K/mTOR inhibitors inhibited phosphorylation of ATR target Chk1 and the mTOR targets S6 and 4EBP1. The lack of induction of γH2Ax despite inhibiting Chk1 phosphorylation is likely because of the fact that they also inhibit ATM, the kinase that phosphorylates H2Ax when DNA double-strand breaks occur after replication fork collapse.[37]

Having established that VE-821 is a selective ATRi we used it to investigate if ATR inhibition synergizes with BETi. Indeed we found that VE-821 synergized with both the prototype BETi JQ1 and the more recently developed RVX2135[21] in a dose-dependent manner (Figure 2c and Supplementary Figures S3a and b). To investigate at which level the anti-lymphoma effect is achieved we performed western blotting and cell cycle analysis using flow cytometry. Combining BETi and ATRi caused robust cell death that correlates with a synergistically enhanced level of PARP cleavage compared with single-agent treatments (Supplementary Figure S3c). Moreover, treatment with BETi induced G1 arrest at high concentrations, whereas VE-821 induced accumulation in G2/M and apoptosis (Figure 2d). We also analyzed levels of γH2Ax; as it is enhanced by ATR inhibition (Figure 2b) and by BETi.[21,38] Indeed, combination treatment synergistically enhances γH2Ax staining (Supplementary Figures S3d and e) but this can be partly blocked by Q-VD-OPH, a pan-caspase inhibitor (Supplementary Figure S3d). It is thus likely that some of the γH2Ax signal is owing to a DNA-damage response triggered by apoptotic DNA fragmentation. Importantly, the ability of VE-821 to synergize with BETi was phenocopied using an inhibitor of Chk1 (AZD7762, Supplementary Figure S4a) or another ATRi (AZ20, Supplementary Figures S4b and c). We therefore conclude that inhibition of the canonical ATR-Chk1 replication stress pathways synergizes with BET inhibition. Finally, three human Burkitt lymphoma cell lines were also sensitive to the combination therapy (Figure 2e) suggesting that there could be therapeutic advantages of combining BETi and ATRi in treatment of lymphoma patients.

RVX2135 and AZ20 synergize *in vivo*

Our data is of therapeutic interest because ATRi, Chk1 inhibitors and BETi are being developed for clinical applications. BETi synergizing with ATR inhibition would imply that ATRi might not need to be combined with genotoxic chemotherapy, which has been rationally assumed.[39] To be able to test this notion in an *in vivo* setting we interrogated the effect of AZ20, which unlike VE-821 is a bioavailable ATRi.[40] To that end, we used a syngeneic tumor transplant model where λ820 cells were injected into the tail vein of mice. Two weeks after transplantation we counted the white blood cells (WBC) and once it was above the normal range (6000–15 000 cells/μl) we divided the mice into four treatment groups. Five days after initiation of treatment, WBC counts were measured. Whereas vehicle-treated mice had a steady increase in WBC count, mice treated with BETi or AZ20 had lower levels, which reached statistical significance in the combination-treated mice (Figure 3a). This translates into a statistically significant prolonged survival (Figure 3b) although the mice eventually succumbed to lymphoma. In previous experiments we noted that RVX2135 did not clear lymphoma efficiently from lymph nodes.[21] Because λ820 cells predominantly form nodular lymphoma, we also tested the combination treatment in mice bearing another Myc-induced lymphoma, the λ2749 line,[21] which has been propagated by serial transplantation *in vivo* and has never been in culture. In this model, the RVX2135/AZ20 combination treatment causes a rapid clearance of the associated lympholeukemia (Figure 3c) and a prolonged survival (Figure 3d). In fact, the effect was so marked that if mice were started on treatment when lymphomas were large enough to be palpable, the mice showed signs of tumor lysis syndrome and a significant reduction in spleen size upon autopsy of the treated mice after just 1 day of treatment (Figure 3e).

BETi and ATRi combination therapy triggers a transcriptional output resembling DNA damage-induced senescence-associated secretory pathway

As shown above, both BETi and ATRi trigger apoptosis and DNA damage that is exacerbated in combination. However, although the synergy was dose-dependent with regards to BETi, effects on transcription could not be excluded. To gain insight into the transcriptional changes we performed Illumina bead array analyses of RNA extracted from λ820 cells treated with RVX2135, VE-821 or both in the presence of the pan-caspase inhibitor Q-VD-OPH to ensure viable cells and inhibit induction of apoptotic gene expression (Supplementary Dataset 1, GEO accession# GSE74873). Principle component analysis of the transcriptome revealed four clearly separated groups (Figure 4a).

To gain insight to how the individual and the combination therapies affected the cells transcriptionally we mined the REACTOME geneset database using geneset enrichment analysis. In VE-821-treated and in RVX2135-treated cells the genesets of replication stress (RVX2135) and chromosome maintenance (VE-821) had the lowest false discovery rate ($q < 0.25$ is regarded highly enriched, Figure 4b). This is in accordance with both of the compounds inhibiting replication. On the other hand, the combination-treated cells had elevated transcript levels of genes involved in senescence-associated secretory pathway, including the NFκB family member Rela (Figures 4b and c). Expanding that to analyze a larger geneset focused on the NFκB pathway (at http://bioinfo.lifl.fr/NF-KB/ and using the Ingenuity pathway analyzer) revealed that several NFκB family members and targets

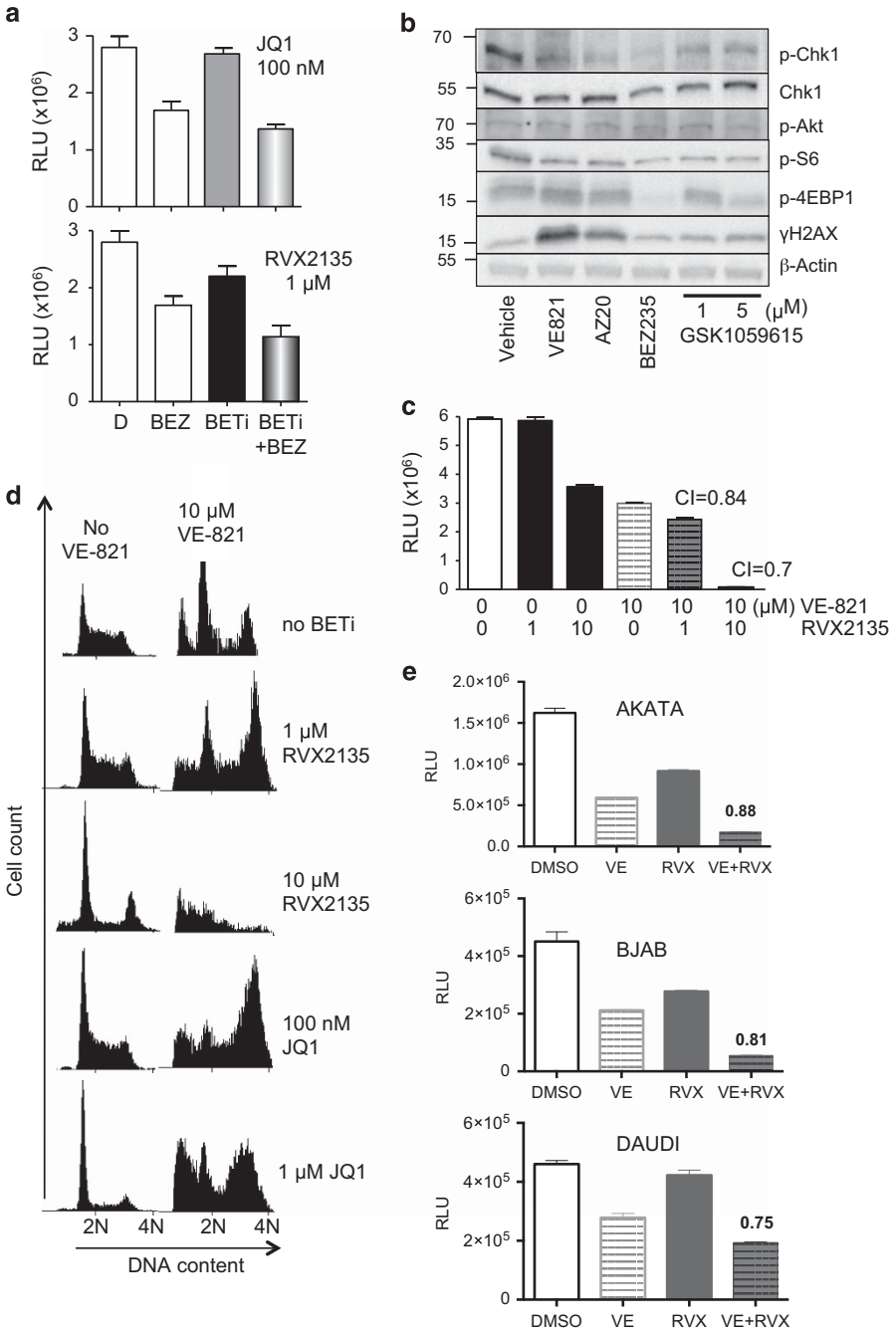

Figure 2. BETi synergize with ATRi to trigger apoptosis of Myc-induced lymphoma cells (**a**) λ820 cells were cultured in the presence of increasing concentrations (100 nM to 10 μM) of BETi and/or the mTOR/PI3K inhibitor NVP-BEZ235 (10 nM to 1 μM) for 24 h and analyzed for viability with Cell-Titer-Glo in a plate luminometer measuring relative luciferase units (RLU). Synergy is observed at the displayed concentrations of 100 nM JQ1/1 μM RVX2135 and 1 μM NVP-BEZ235; at all other concentrations the combination treatment was additive. (**b**) Western blotting analysis of lysates from λ820 cells treated with vehicle (0.1% DMSO), 10 μM of the ATR inhibitor VE-821, 1 μM of ATR inhibitor AZ20, 1 μM PI3K/mTOR inhibitor NVP-BEZ235 or indicated concentrations of PI3K/mTOR inhibitor GSK1059615. (**c**) λ820 cells were cultured in the presence of DMSO, 1 or 10 μM of RVX2135 (RVX) and/or the ATR inhibitor VE-821 (VE; 10 μM) for 24 h and analyzed for viability with Cell-Titer-Glo. Synergy score (combination index, CI) is shown. A value below 1.0 demonstrates synergy. (**d**) Cell cycle distribution of cells treated with VE-821 and BETi at indicated concentrations for 24 h. (**e**) Cell-Titer-Glo viability measurements of human B-cell lymphoma cell lines Akata, Daudi and BJAB treated with 10 μM RVX2135 (RVX) alone or in combination with 10 μM ATRi VE-821 (VE). Combination index is shown above the bar of the combination treatment.

were induced in RVX2135/VE-821-treated lymphoma cells (Figure 4d and Supplementary Figure S5). This is of particular interest as some of us have shown previously that most components of NFκB signaling normally are suppressed in Myc-induced murine lymphoma.[41–43] On the other hand, the NFκB pathway, senescence-associated secretory pathway, ER stress and autophagy have been previously implicated in responses of Myc-induced lymphoma to DNA-damaging drugs.[44–46] We thus also investigated key mediators of these pathways. The expression of DDIT3/CHOP and ATF4, mediators of ER stress, and the

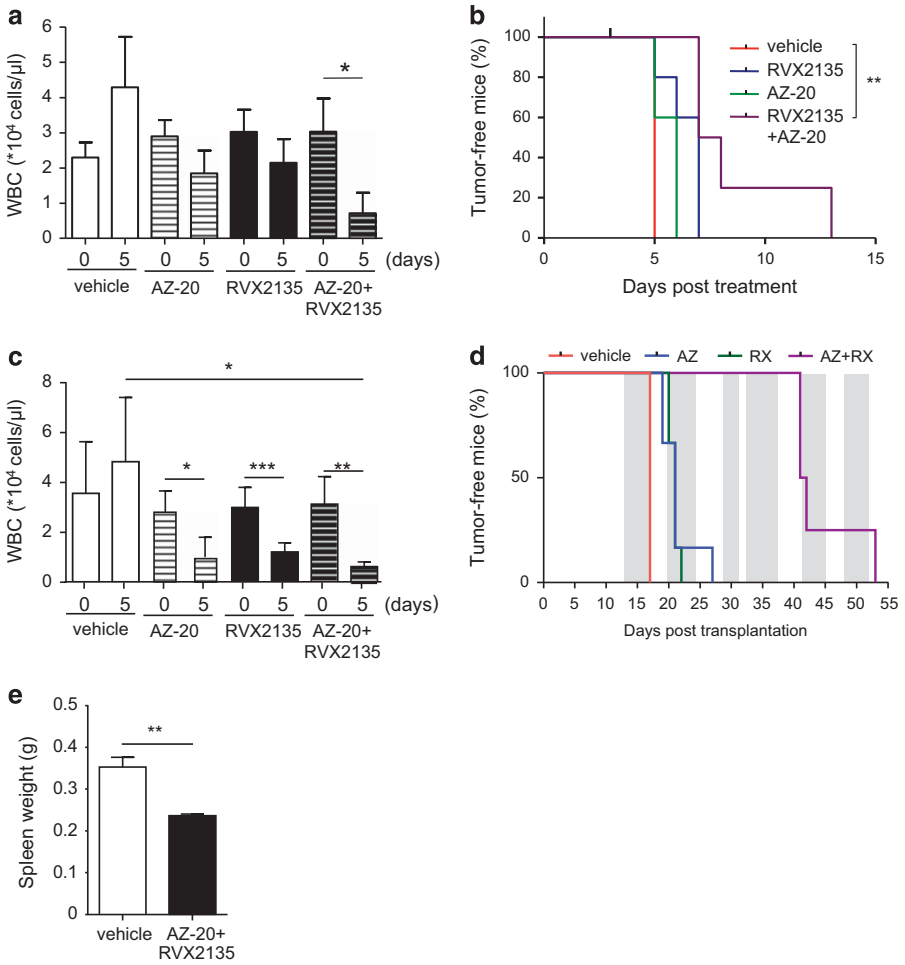

Figure 3. BETi synergize with ATRi to trigger apoptosis and increased survival of lymphoma-bearing mice. (**a**) λ820 cells were transplanted into B6 mice via tail vein injection. The peripheral white blood cell (WBC) count was monitored and when the levels reached that of the leukemic phase of lymphoma development (>15 000 cells/μl) mice were randomized and treatment was commenced. Five days after initiation of treatment with vehicle, AZ20, RVX2135 or a combination of both, WBC counts were monitored again. (**b**) Kaplan–Meier curve of mice carrying λ820 lymphoma cells treated with indicated compounds. All treatments resulted in a statistically significant delay in tumor onset (vehicle vs AZ20—*P*-value = 0.0103; vehicle vs RVX2135—*P*-value = 0.0201; vehicle vs RVX2135+AZ20 combination—*P*-value = 0.0036). (**c**) #2749, a lymphoma model that has been maintained as an *in vivo* propagated line, were transplanted into B6 mice via tail vein injection. WBC count was monitored and when the levels reached that of the leukemic phase of lymphoma development mice were randomized and treatment was commenced. Five days after initiation of treatment with vehicle, AZ20, RVX2135 or a combination of both, WBC counts were monitored again. (**d**) Kaplan–Meier curve of mice carrying #2749 lymphoma cells treated with the indicated compounds. All treatments resulted in a statistically significant delay in tumor onset (vehicle vs AZ20—*P*-value = 0.0009; vehicle vs RVX2135—*P*-value = 0.0009; vehicle vs RVX2135 +AZ20 combination—*P*-value = 0.0016). (**e**) Spleen weights of mice 24 h after treatment with three doses of vehicle or two doses of RVX2135 and one dose with AZ20.

senescence-associated cytokines Cxcl1 and Cxcl2 were induced by VE-821 or the combination treatment (Figures 4e and f and Supplementary Figures S6a and b). Moreover, the p62 protein, which is degraded by autophagy,[47] was induced by both RVX2135 and VE-821 but exhibited even stronger expression in combination-treated cells in both mouse λ820 cells and in the Daudi human Burkitt lymphoma cells (Figures 4e and f). Surprisingly though, LC3 cleavage was not altered, suggesting that p62 accumulation was not because of blocked autophagy. On the other hand, p62 also operates as a positive signaling adapter and target of NFκB signaling.[47–49] Indeed, the mRNA levels of p62 were induced by VE-821 and the combination treatment (Supplementary Figures S6a and b), likely explaining the increase in protein levels (Figures 4e and f). Taken together, our data suggest an engagement of NFκB signaling in cells undergoing BET and ATR inhibitor combination treatment. Future studies are warranted that will address the earliest events resulting in the activation of NFκB signaling and whether or not the pathway is involved in cell survival or cell death.

DISCUSSION

Here we show that BETi and ATRi synergize to kill cancer cells both *in vitro* and *in vivo*. The rapid therapeutic effect of the combination treatment is unprecedented in our lab when using targeted agents in lymphoma. The treatment combination was well tolerated when given to mice with low tumor load. However, future studies need to address several questions arising from this work. Is the combination therapy tumor-selective and thus safer than classic chemotherapy? The robust cell death is certainly similar but additional safety data is warranted. For instance, how will the immune system and normal stem cells respond to this treatment? With the advancements in immune-oncology therapies it is of great interest to assess the potential for combinations

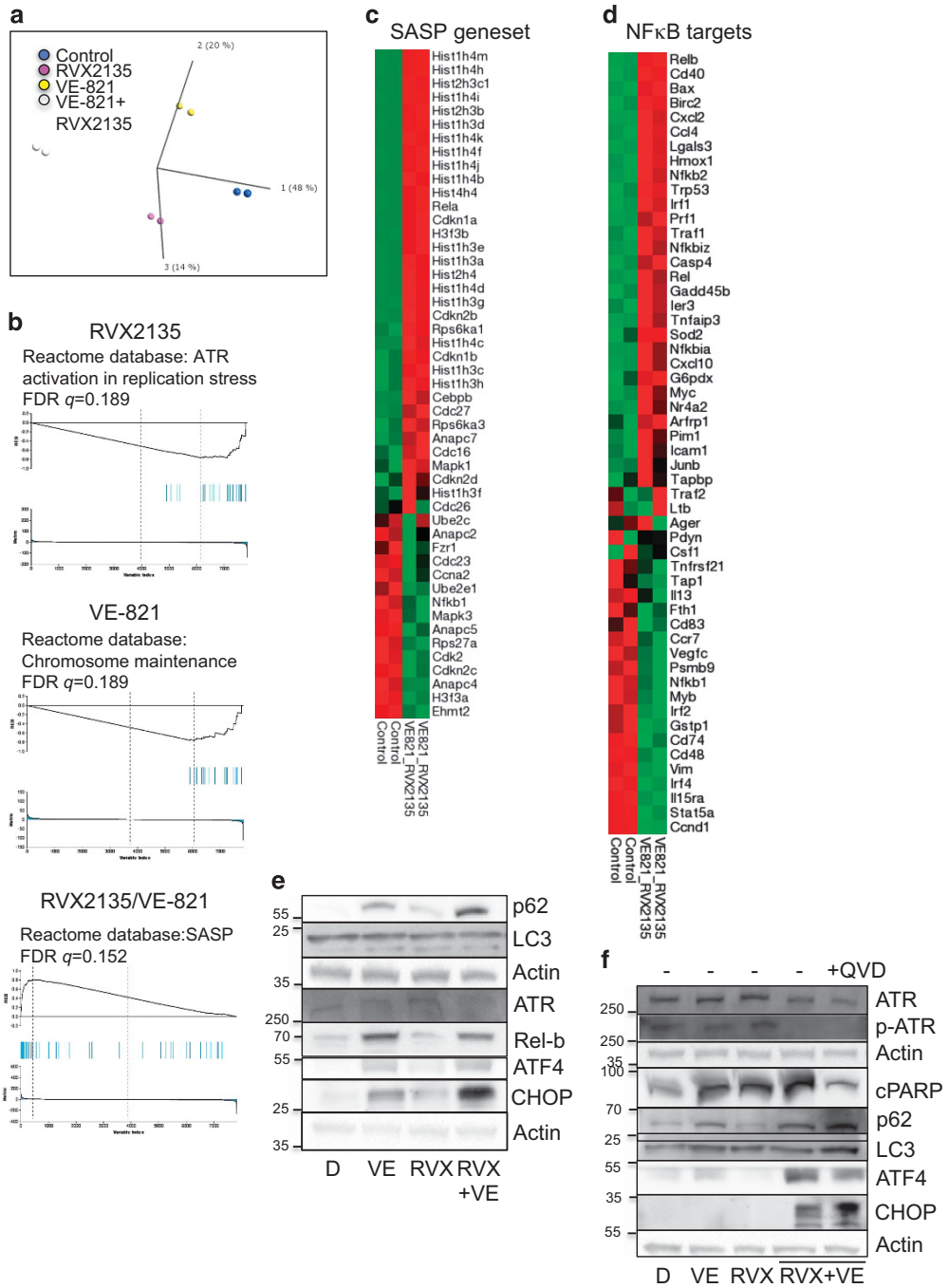

Figure 4. BETi and ATRi block transcription of genes involved in replication but induce genes involved in senescence-associated secretory pathway and ER stress. RNA was prepared from λ820 cells treated with vehicle (0.1% DMSO), 10 μM RVX2135, 10 μM VE-821 or both RVX2135 and VE-821, all in the presence of 10 μM Q-VD-OPH to block apoptosis during 24 h. (**a**) Principle component analysis (PCA) of the transcriptomes of the indicated treatment groups. (**b**) GSEA analysis of the REACTOME database. Shown are the genesets with the lowest false discovery rates ($q < 0.25$). (**c**) Clustering analysis of the senescence-associated secretory pathway (SASP) geneset from the REACTOME database. (**d**) Clustering analysis of a geneset containing NFκB target genes. (**e**) Western blot (WB) analysis of λ820 cells treated with vehicle (0.1% DMSO), 10 μM RVX2135, 10 μM VE-821 or both RVX2135 and VE-821, all in the presence of 10 μM Q-VD-OPH to block apoptosis during 24 h. Actin was used as a loading control. (**f**) WB analysis of Daudi cells treated with vehicle (0.1% DMSO), 10 μM RVX2135, 10 μM VE-821 or both RVX2135 and VE-821, in the absence or presence of 1 μM Q-VD-OPH to block apoptosis during 24 h.

with new agents. In this regard, some questions have already been raised about BETi in preclinical models[50,51] and we will learn much more from the multiple ongoing BETi oncology clinical trials.

Additional questions arise regarding the mechanism behind the observed effects. It will be essential to first define if (i) ATRi potentiates the effect of BETi, (ii) whether BETi potentiates the effects of ATRi or (iii) if a synthetic lethality situation is at play. Defining key components at the replication fork upon replication stress has very recently been possible via unbiased proteomics approaches.[52] It is noteworthy that some components regulated by ATR during replication stress such as RFC1, DNA-PK and CAF1 have previously been found to interact with BRD4 and BRD2.[53,54]

Furthermore, a short isoform of BRD4 has been shown to insulate H2Ax from excess and unspecific ATM phosphorylation.[38] It is possible to envision that a 'pseudo-DNA damage signal' could elicit problems during replication that might require ATR to resolve. Finally, our own data here points to that NFκB signaling, a normally silenced transcription factor network in Myc-induced lymphoma,[41–43] become reactivated in cells treated with ATRi/BETi. It is tempting to speculate that ATR could regulate transcription by phosphorylating a transcription factor that could operate together with displaced BET proteins to regulate NFκB signaling. This would represent a truly synergistic lethal effect that could only be observed during this particular combination. A candidate transcription factor for this event is MIZ1 as it is regulated during replication fork stalling by UV[55] and because it has been shown to stimulate the transcription of NFκB2.[41] However, although the NFκB family member RelA is acetylated and requires binding to Brd4,[56,57] a full understanding of the events likely requires multiple lines of future investigations.

Currently, several BET inhibitors such as OTX015, GSK525762, BAY1238097, TEN-010, BMS-986158 and CPI-0610, and ATR inhibitors such as AZD6738 and VX-970 are completing phase I/II clinical trials as cancer monotherapies (https://clinicaltrials.gov). Identification of appropriate combination therapies is of high interest. That ATRi combined with BETi can synergize to induce lymphoma cell death without the use of genotoxic drugs could represent a significant advantage.

MATERIALS AND METHODS

Inhibitors and chemical library

JQ1 was purchased from Cayman chemicals (Ann Arbor, MI, USA) and RVX2135 was a kind gift from Zenith Epigenetics (Calgary, AB, Canada). ATR inhibitors, AZ20 and VE-821 are commercially available at AXON Medchem (Groningen, The Netherlands) and MedChem Express (Princeton, NJ, USA), respectively. Pan-caspase inhibitor, Q-VD-OPH was procured from Sigma-Aldrich (St Louis, MO, USA). All the inhibitors were dissolved in DMSO and stored at − 20 °C. The Chk1 inhibitor AZD7762 and the pharmacogenetic library was purchased from Selleck chemicals (Houston, TX, USA) and have been described before.[24]

In vivo mouse experiments

All animal experiments were performed in accordance with regional/local animal ethics committee approval (approval numbers 287/2011, 288/2011 and 36/14). C57BL/6-Tyr (albino) syngenic mice were transplanted with lymphoma cells and were followed by measuring WBC counts in blood samples from the saphenous vein. When >15 cells/nl were reached in all mice they were divided into groups so as to ensure a similar spread in WBC in all groups. They were thereafter treated with oral RVX2135 at 75 mg/kg b.i.d. ($n=5$) and/or ip AZ20 at 50 mg/kg q.d. ($n=5$). Control mice ($n=4$) received oral and ip vehicle (10% PEG300, 2.5% Tween-80, pH 4). Blood samples were collected 5 days post treatment. Mice were scored sick and killed when palpable lymphomas appeared. Neither the animal technician performing the dosing nor the investigators scoring the mice were blinded to the experiment.

Cell culture

All B-cell lines were cultured in RPMI supplemented with 10% fetal bovine serum, stable glutamine, 50 μM of β-mercaptoethanol. λ820 and λ663 cell lines were established by serial culturing of lymphomas that arose in λ-*Myc* mice and Eμ239 was established similarly from Eμ-Myc mouse. Akata, Daudi and BJAB were lab stocks that were routinely confirmed to be Myc-driven B-cell lymphoma lines by qRT-PCR or western blotting of human c-Myc. P493-6 cells were kindly provided by G Bornkamm (Munich, Germany) and were cultured and treated with tetracycline (Sigma-Aldrich) as previously described.[23] All cell lines were confirmed to be mycoplasma-free by standard PCR analysis.

Cell viability and cell cycle analysis

Lymphoma cells were collected by centrifugation and were lysed and stained in modified Vindelov's solution (20 mM Tris pH 8.0, 100 mM NaCl, 1 μg/ml 7-AAD, 20 μg/ml RNase and 0.1% NP40) for 30 min at 37 °C. DNA content was analyzed on a BD Accuri C6 (Becton-Dickinson, Durham, NC, USA) using the FL3 channel in linear scale for S-Phase measurements, and in logarithmic scale for sub-G1 measurements (apoptosis).

For measurement of DNA synthesis in S-phase, cells were plated into 96-well plates and cultured in the presence of vehicle (DMSO), JQ1 or RVX2135. Cells were incubated with ^{3}H-thymidine for the final 4 h of treatment and subsequently collected onto glass fiber filters and counted in a TopCount scintillation counter (Perkin-Elmer, Norwalk, CT, USA).

For cell viability measurements (drug screening and synergy experiments) cells were cultured in 96-well plates and metabolic activity was measured using the ATP-based Cell-Titer-Glo assay (Promega, Madison, WI, USA) in a VICTOR plate luminometer (Perkin-Elmer).

RNA analyses

For qRT-PCR, RNA from was isolated using NucleoSpin RNA II kit (Macherey-Nagel, Düren, Germany). After quantification, 500 ng of RNA was converted to cDNA using the iScript cDNA synthesis kit (Bio-Rad, Hercules, CA, USA). qRT-PCR was performed using KAPA SYBR FAST ABI Prism 2X qPCR Master Mix (Kapa Biosystems, Woburn, MA, USA). Data analyses were performed by comparing the ΔΔCt values with a control sample set as 1.

Expression profiling using Illumina (San Diego, CA, USA) Mouse RefSeq bead arrays was essentially performed as previously described[21] and the data has been deposited at NCBI Gene Expression Omnibus (GEO accession# GSE74873). Principle component analysis and geneset enrichment analysis were performed using the Qlucore software (Qlucore, Lund, Sweden) and clustering analyses were performed using Qlucore or GENE-E. Additional pathway analyses were done using the Ingenuity pathway analyzer (Qiagen, Redwood City, CA, USA).

Immunoblotting

Cell pellets were lysed in lysis buffer as described before.[34] In all, 50 μg of protein was resolved on 4–20% ClearPAGE gels (C.B.S. Scientific Company, San Diego, CA, USA) and transferred to nitrocellulose membrane (Protran, GE Healthcare Bio-Sciences, Piscataway, NJ, USA). The membrane was blotted with specific antibodies. Antibodies against the following proteins were used: Myc, p-ATR, p-Chk1, p-4EBP1, p-AKT, p-S6 (Cell Signaling Technology, Danvers, MA, USA), Geminin, c-Rel, Rel-B, Chk1, CHOP, ATR, ATF4 (Santa Crutz Biotechnology, Dallas, TX, USA), p62 (Progen Biotechnik, Heidelberg, Germany), LC3 (Novus Biologicals, Littleton, CO, USA), Actin (Sigma-Aldrich).

Statistical analysis

The bars shown represent the mean ± s.d. Combination indices (CI) between drug A and B was calculated using the formula CI = expected additive/observed; where, expected additive = 1 − (value of drug A/vehicle × value of drug B/vehicle). Value <1 is considered synergistic, Value = 1 is additive and value >1 is antagonistic. All cell culture experiments were repeated thrice, the microarray was performed on two biological replicates and the animal studies had a minimum of four animals per group. The two-tailed Student's *t*-test or tumor-free survival (log-rank) analyses were performed using GraphPad Prism (GraphPad Software, La Jolla, CA, USA). $^{*}P<0.05$, $^{**}P<0.01$, $^{***}P<0.001$ and $^{****}P<0.0001$.

CONFLICT OF INTEREST

KGM was an employee of Zenith Epigenetics Corp at the begining of this project. The remaining authors declare no conflict of interest.

ACKNOWLEDGEMENTS

We thank Sofia Nordstrand for animal care, and Eric Campeau and Zenith Epigenetics for RVX2135 and helpful discussions. This work was supported by grants from the Swedish Cancer Society, the Swedish Research Council, the Region Västra Götaland (Sahlgrenska University Hospital, Gothenburg), the Knut and Alice Wallenberg Foundation, the Sahlgrenska Academy and BioCARE—a National Strategic Cancer Research Program at University of Gothenburg (to JAN), and from the Assar Gabrielsson Foundation and the W&M Lundgren Foundation (to SVM, JB and LCG).

REFERENCES

1 Belkina AC, Denis GV. BET domain co-regulators in obesity, inflammation and cancer. *Nat Rev Cancer* 2012; **12**: 465–477.
2 Sinha A, Faller DV, Denis GV. Bromodomain analysis of Brd2-dependent transcriptional activation of cyclin A. *Biochem J* 2005; **387**: 257–269.
3 Denis GV, Vaziri C, Guo N, Faller DV. RING3 kinase transactivates promoters of cell cycle regulatory genes through E2F. *Cell Growth Differ* 2000; **11**: 417–424.
4 Jang MK, Mochizuki K, Zhou M, Jeong HS, Brady JN, Ozato K. The bromodomain protein Brd4 is a positive regulatory component of P-TEFb and stimulates RNA polymerase II-dependent transcription. *Mol Cell* 2005; **19**: 523–534.
5 Yang Z, Yik JH, Chen R, He N, Jang MK, Ozato K *et al.* Recruitment of P-TEFb for stimulation of transcriptional elongation by the bromodomain protein Brd4. *Mol Cell* 2005; **19**: 535–545.
6 Marshall NF, Peng J, Xie Z, Price DH. Control of RNA polymerase II elongation potential by a novel carboxyl-terminal domain kinase. *J Biol Chem* 1996; **271**: 27176–27183.
7 Loven J, Hoke HA, Lin CY, Lau A, Orlando DA, Vakoc CR *et al.* Selective inhibition of tumor oncogenes by disruption of super-enhancers. *Cell* 2013; **153**: 320–334.
8 Venkataraman S, Alimova I, Balakrishnan I, Harris P, Birks DK, Griesinger A *et al.* Inhibition of BRD4 attenuates tumor cell self-renewal and suppresses stem cell signaling in MYC driven medulloblastoma. *Oncotarget* 2014; **5**: 2355–2371.
9 Pastori C, Daniel M, Penas C, Volmar CH, Johnstone AL, Brothers SP *et al.* BET bromodomain proteins are required for glioblastoma cell proliferation. *Epigenetics* 2014; **9**: 611–620.
10 Loosveld M, Castellano R, Gon S, Goubard A, Crouzet T, Pouyet L *et al.* Therapeutic targeting of c-Myc in T-cell acute lymphoblastic leukemia, T-ALL. *Oncotarget* 2014; **5**: 3168–3172.
11 Bandopadhayay P, Bergthold G, Nguyen B, Schubert S, Gholamin S, Tang Y *et al.* BET bromodomain inhibition of MYC-amplified medulloblastoma. *Clin Cancer Res* 2014; **20**: 912–925.
12 Asangani IA, Dommeti VL, Wang X, Malik R, Cieslik M, Yang R *et al.* Therapeutic targeting of BET bromodomain proteins in castration-resistant prostate cancer. *Nature* 2014; **510**: 278–282.
13 Tolani B, Gopalakrishnan R, Punj V, Matta H, Chaudhary PM. Targeting Myc in KSHV-associated primary effusion lymphoma with BET bromodomain inhibitors. *Oncogene* 2013; **33**: 2928–2937.
14 Puissant A, Frumm SM, Alexe G, Bassil CF, Qi J, Chanthery YH *et al.* Targeting MYCN in neuroblastoma by BET bromodomain inhibition. *Cancer Discov* 2013; **3**: 308–323.
15 Gao L, Schwartzman J, Gibbs A, Lisac R, Kleinschmidt R, Wilmot B *et al.* Androgen receptor promotes ligand-independent prostate cancer progression through c-Myc upregulation. *PLoS One* 2013; **8**: e63563.
16 Cheng Z, Gong Y, Ma Y, Lu K, Lu X, Pierce LA *et al.* Inhibition of BET bromodomain targets genetically diverse glioblastoma. *Clin Cancer Res* 2013; **19**: 1748–1759.
17 Mertz JA, Conery AR, Bryant BM, Sandy P, Balasubramanian S, Mele DA *et al.* Targeting MYC dependence in cancer by inhibiting BET bromodomains. *Proc Natl Acad Sci USA* 2011; **108**: 16669–16674.
18 Delmore JE, Issa GC, Lemieux ME, Rahl PB, Shi J, Jacobs HM *et al.* BET bromodomain inhibition as a therapeutic strategy to target c-Myc. *Cell* 2011; **146**: 904–917.
19 Keene RG, Mueller A, Landick R, London L. Transcriptional pause, arrest and termination sites for RNA polymerase II in mammalian N- and c-myc genes. *Nucleic Acids Res* 1999; **27**: 3173–3182.
20 Kerppola TK, Kane CM. Intrinsic sites of transcription termination and pausing in the c-myc gene. *Mol Cell Biol* 1988; **8**: 4389–4394.
21 Bhadury J, Nilsson LM, Muralidharan SV, Green LC, Li Z, Gesner EM *et al.* BET and HDAC inhibitors induce similar genes and biological effects and synergize to kill in Myc-induced murine lymphoma. *Proc Natl Acad Sci USA* 2014; **111**: E2721–E2730.
22 Fiskus W, Sharma S, Qi J, Valenta JA, Schaub LJ, Shah B *et al.* Highly active combination of BRD4 antagonist and histone deacetylase inhibitor against human acute myelogenous leukemia cells. *Mol Cancer Ther* 2014; **13**: 1142–1154.
23 Pajic A, Spitkovsky D, Christoph B, Kempkes B, Schuhmacher M, Staege MS *et al.* Cell cycle activation by c-myc in a burkitt lymphoma model cell line. *Int J Cancer* 2000; **87**: 787–793.
24 Bhadury J, Lopez MD, Muralidharan SV, Nilsson LM, Nilsson JA. Identification of tumorigenic and therapeutically actionable mutations in transplantable mouse tumor cells by exome sequencing. *Oncogenesis* 2013; **2**: e44.
25 Ember SW, Zhu JY, Olesen SH, Martin MP, Becker A, Berndt N *et al.* Acetyl-lysine binding site of bromodomain-containing protein 4 (BRD4) interacts with diverse kinase inhibitors. *ACS Chem Biol* 2014; **9**: 1160–1171.
26 Ciceri P, Muller S, O'Mahony A, Fedorov O, Filippakopoulos P, Hunt JP *et al.* Dual kinase-bromodomain inhibitors for rationally designed polypharmacology. *Nat Chem Biol* 2014; **10**: 305–312.
27 Dey A, Chitsaz F, Abbasi A, Misteli T, Ozato K. The double bromodomain protein Brd4 binds to acetylated chromatin during interphase and mitosis. *Proc Natl Acad Sci USA* 2003; **100**: 8758–8763.
28 Boi M, Gaudio E, Bonetti P, Kwee I, Bernasconi E, Tarantelli C *et al.* The BET bromodomain inhibitor OTX015 affects pathogenetic pathways in preclinical B-cell tumor models and synergizes with targeted drugs. *Clin Cancer Res* 2015; **21**: 1628–1638.
29 Stratikopoulos EE, Dendy M, Szabolcs M, Khaykin AJ, Lefebvre C, Zhou MM *et al.* Kinase and BET inhibitors together clamp inhibition of PI3K signaling and overcome resistance to therapy. *Cancer Cell* 2015; **27**: 837–851.
30 Lecona E, Fernandez-Capetillo O. Replication stress and cancer: it takes two to tango. *Exp Cell Res* 2014; **329**: 26–34.
31 Ferrao PT, Bukczynska EP, Johnstone RW, McArthur GA. Efficacy of CHK inhibitors as single agents in MYC-driven lymphoma cells. *Oncogene* 2012; **31**: 1661–1672.
32 Murga M, Campaner S, Lopez-Contreras AJ, Toledo LI, Soria R, Montana MF *et al.* Exploiting oncogene-induced replicative stress for the selective killing of Myc-driven tumors. *Nat Struct Mol Biol* 2011; **18**: 1331–1335.
33 Höglund A, Strömvall K, Li Y, Forshell LP, Nilsson JA. Chk2 deficiency in Myc overexpressing lymphoma cells elicits a synergistic lethal response in combination with PARP inhibition. *Cell Cycle* 2011; **10**: 3598–3607.
34 Höglund A, Nilsson L, Muralidharan SV, Hasvold LA, Merta P, Rudelius M *et al.* Therapeutic implications for the induced levels of Chk1 in Myc-expressing cancer cells. *Clin Cancer Res* 2011; **17**: 7067–7079.
35 Shortt J, Martin BP, Newbold A, Hannan KM, Devlin JR, Baker AJ *et al.* Combined inhibition of PI3K-related DNA damage response kinases and mTORC1 induces apoptosis in MYC-driven B-cell lymphomas. *Blood* 2013; **121**: 2964–2974.
36 Toledo LI, Murga M, Zur R, Soria R, Rodriguez A, Martinez S *et al.* A cell-based screen identifies ATR inhibitors with synthetic lethal properties for cancer-associated mutations. *Nat Struct Mol Biol* 2011; **18**: 721–727.
37 Reaper PM, Griffiths MR, Long JM, Charrier JD, Maccormick S, Charlton PA *et al.* Selective killing of ATM- or p53-deficient cancer cells through inhibition of ATR. *Nat Chem Biol* 2011; **7**: 428–430.
38 Floyd SR, Pacold ME, Huang Q, Clarke SM, Lam FC, Cannell IG *et al.* The bromodomain protein Brd4 insulates chromatin from DNA damage signalling. *Nature* 2013; **498**: 246–250.
39 Josse R, Martin SE, Guha R, Ormanoglu P, Pfister TD, Reaper PM *et al.* ATR inhibitors VE-821 and VX-970 sensitize cancer cells to topoisomerase i inhibitors by disabling DNA replication initiation and fork elongation responses. *Cancer Res* 2014; **74**: 6968–6979.
40 Foote KM, Blades K, Cronin A, Fillery S, Guichard SS, Hassall L *et al.* Discovery of 4-{4-[(3R)-3-Methylmorpholin-4-yl]-6-[1-(methylsulfonyl)cyclopropyl]pyrimidin-2-y l}-1H-indole (AZ20): a potent and selective inhibitor of ATR protein kinase with monotherapy *in vivo* antitumor activity. *J Med Chem* 2013; **56**: 2125–2138.
41 Keller U, Huber J, Nilsson JA, Fallahi M, Hall MA, Peschel C *et al.* Myc suppression of Nfkb2 accelerates lymphomagenesis. *BMC Cancer* 2010; **10**: 348.
42 Klapproth K, Sander S, Marinkovic D, Baumann B, Wirth T. The IKK2/NF-{kappa}B pathway suppresses MYC-induced lymphomagenesis. *Blood* 2009; **114**: 2448–2458.
43 Keller U, Nilsson JA, Maclean KH, Old JB, Cleveland JL. Nfkb 1 is dispensable for Myc-induced lymphomagenesis. *Oncogene* 2005; **24**: 6231–6240.
44 Dorr JR, Yu Y, Milanovic M, Beuster G, Zasada C, Dabritz JH *et al.* Synthetic lethal metabolic targeting of cellular senescence in cancer therapy. *Nature* 2013; **501**: 421–425.
45 Jing H, Kase J, Dorr JR, Milanovic M, Lenze D, Grau M *et al.* Opposing roles of NF-kappaB in anti-cancer treatment outcome unveiled by cross-species investigations. *Genes Dev* 2011; **25**: 2137–2146.
46 Chien Y, Scuoppo C, Wang X, Fang X, Balgley B, Bolden JE *et al.* Control of the senescence-associated secretory phenotype by NF-kappaB promotes senescence and enhances chemosensitivity. *Genes Dev* 2011; **25**: 2125–2136.
47 Moscat J, Diaz-Meco MT. p62 at the crossroads of autophagy, apoptosis, and cancer. *Cell* 2009; **137**: 1001–1004.
48 Fang J, Barker B, Bolanos L, Liu X, Jerez A, Makishima H *et al.* Myeloid malignancies with chromosome 5q deletions acquire a dependency on an intrachromosomal NF-kappaB gene network. *Cell Rep* 2014; **8**: 1328–1338.
49 Sanz L, Diaz-Meco MT, Nakano H, Moscat J. The atypical PKC-interacting protein p62 channels NF-kappaB activation by the IL-1-TRAF6 pathway. *EMBO J* 2000; **19**: 1576–1586.

50 Stanlie A, Yousif AS, Akiyama H, Honjo T, Begum NA. Chromatin reader Brd4 functions in Ig class switching as a repair complex adaptor of nonhomologous end-joining. *Mol Cell* 2014; **55**: 97–110.
51 Bolden JE, Tasdemir N, Dow LE, van Es JH, Wilkinson JE, Zhao Z *et al.* Inducible *in vivo* silencing of Brd4 identifies potential toxicities of sustained BET protein inhibition. *Cell Rep* 2014; **8**: 1919–1929.
52 Tang C, Wang X, Soh H, Seyedin S, Cortez MA, Krishnan S *et al.* Combining radiation and immunotherapy: a new systemic therapy for solid tumors? *Cancer Immunol Res* 2014; **2**: 831–838.
53 Denis GV, McComb ME, Faller DV, Sinha A, Romesser PB, Costello CE. Identification of transcription complexes that contain the double bromodomain protein Brd2 and chromatin remodeling machines. *J Proteome Res* 2006; **5**: 502–511.
54 Maruyama T, Farina A, Dey A, Cheong J, Bermudez VP, Tamura T *et al.* A mammalian bromodomain protein, brd4, interacts with replication factor C and inhibits progression to S phase. *Mol Cell Biol* 2002; **22**: 6509–6520.
55 Herold S, Wanzel M, Beuger V, Frohme C, Beul D, Hillukkala T *et al.* Negative regulation of the mammalian UV response by Myc through association with Miz-1. *Mol Cell* 2002; **10**: 509–521.
56 Zou Z, Huang B, Wu X, Zhang H, Qi J, Bradner J *et al.* Brd4 maintains constitutively active NF-kappaB in cancer cells by binding to acetylated RelA. *Oncogene* 2013; **33**: 2395–2404.
57 Huang B, Yang XD, Zhou MM, Ozato K, Chen LF. Brd4 coactivates transcriptional activation of NF-kappaB via specific binding to acetylated RelA. *Mol Cell Biol* 2009; **29**: 1375–1387.

Supplementary Information accompanies this paper on the Oncogene website (http://www.nature.com/onc)